

# Bayesian co-estimation of selfing rate and locus-specific mutation rates for a partially selfing population

*Benjamin D. Redelings, Seiji Kumagai, Andrei Tatarenkov, Ann K. Sakai, Stephen G. Weller, John C. Avise, and Marcy K. Uyenoyama*

## Abstract

We present a Bayesian method for characterizing the mating system of populations reproducing through a mixture of self-fertilization and random outcrossing. Our method uses patterns of genetic variation across the genome as a basis for inference about pure hermaphroditism, androdioecy, and gynodioecy. We extend the standard coalescence model to accommodate these mating systems, accounting explicitly for multilocus identity disequilibrium, inbreeding depression, and variation in fertility among mating types. We incorporate the Ewens Sampling Formula (ESF) under the infinite-alleles model of mutation to obtain a novel expression for the likelihood of mating system parameters. Our Markov chain Monte Carlo (MCMC) algorithm assigns locus-specific mutation rates, drawn from a common mutation rate distribution that is itself estimated from the data using a Dirichlet Process Prior (DPP) model. Among the parameters jointly inferred are the population-wide rate of self-fertilization, locus-specific mutation rates, and the number of generations since the most recent outcrossing event for each sampled individual.

## 1 Introduction

Inbreeding has pervasive consequences throughout the genome, affecting relationships between genes at each locus and among loci. This generation of genome-wide, multilocus disequilibria of various orders transforms the context in which evolution proceeds. Here, we address a simple form of inbreeding: a mixture of self-fertilization (selfing) and random outcrossing (Clegg, 1980; Ritland, 2002).

Wright's (1921) fundamental method bases the estimation of selfing rates on the coefficient of inbreeding ( $F_{IS}$ ), which reflects the departure from Hardy-Weinberg proportions of genotypes for a given set of allele frequencies. The maximum likelihood method of Enjalbert and David (2000) detects inbreeding from departures of multiple loci from Hardy-Weinberg proportions, accounting for correlations in heterozygosity among loci (identity disequilibrium, Cockerham and Weir, 1968) and estimating allele frequencies for each locus. David et al. (2007) extend the approach of Enjalbert and David (2000), basing the estimation of selfing rates on the distribution of heterozygotes across multiple, unlinked loci, while accom-

modating errors in scoring heterozygotes as homozygotes. A primary objective of **InStruct** (Gao et al., 2007) is the estimation of admixture. It extends the widely-used program **structure** (Pritchard et al., 2000), which bases the estimation of admixture on disequilibria of various forms, by accounting for disequilibria due to selfing. Progeny array methods (see Ritland, 2002), which base the estimation of selfing rates on the genetic analysis of progeny for which one or more parents are known, are particularly well-suited to plant populations. Wang et al. (2012) extend this approach to a random sample of individuals by reconstructing sibship relationships within the sample.

Methods that base the estimation of inbreeding rates on the observed departure from random union of gametes require information on expected Hardy-Weinberg proportions. Population-wide frequencies of alleles observed in a sample ( $\{p_i\}$ ) can be estimated jointly in a maximum-likelihood framework (*e.g.*, Hill et al., 1995) or integrated out as nuisance parameters in a Bayesian framework (*e.g.*, Ayres and Balding, 1998). Similarly, locus-specific heterozygosity ( $1 - \sum p_i^2$ ) can be obtained from observed allele frequencies (Enjalbert and David, 2000) or estimated directly and jointly with the selfing rate (David et al., 2007).

In contrast, our Bayesian method for the analysis of partial self-fertilization derives from a coalescence model that accounts for genetic variation and uses the Ewens Sampling Formula (ESF, Ewens, 1972). Our approach replaces the estimation of allele frequencies ( $\{p_i\}$ ) or heterozygosity ( $1 - \sum p_i^2$ ) by the estimation of a locus-specific mutation rate ( $\theta^*$ ) under the infinite-alleles model of mutation. We use a Dirichlet Process Prior (DPP) to determine the number of classes of mutation rates, the mutation rate for each class, and the class membership of each locus. We assign the DPP parameters in a conservative manner so that it creates a new mutational class only if sufficient evidence exists to justify doing so. Further, while other methods assume that the frequency in the population of an allelic class distinct from those observed in the sample is zero, the ESF provides the probability, under the infinite-alleles model of mutation, that the next-sampled gene represents a novel allele (see (20)).

The ESF provides the exact probability of the allele frequency spectrum observed at a single locus. To determine the probability of the observed frequency spectrum of diploid genotypes at multiple unlinked loci, we determine the distributions of the allele frequency spectra ancestral to the sample at the most recent point at which all sampled gene lineages at each locus reside in separate individuals. In tracing multilocus diploid genotypes back in time, we account for identity disequilibrium (Cockerham and Weir, 1968), the correlation in heterozygosity across loci reflecting that all loci within an individual share their most recent outcrossing event, even in the absence of linkage. Conditional on the number of generations since this event, the genealogical histories of unlinked loci are independent. Our method infers the number of consecutive generations of self-fertilization in the immediate ancestry of each sampled diploid individual and the probability of coalescence during this period between the lineages at each locus.

In addressing pure hermaphroditism, androdioecy (hermaphrodites and males), and gynodioecy (hermaphrodites and females), our method provides a means for the simultaneous inference of various aspects of the mating system, including population-wide rates of self-fertilization, levels of inbreeding depression, and the number of generations since the last random outcrossing event in the ancestry of each individual in the sample. We apply our method to simulated data sets to demonstrate level of accuracy in parameter estimates and

level of confidence. We also apply it to microsatellite data from a self-fertilizing vertebrate (the androdioecious killifish *Kryptolebias marmoratus*) and to gynodioecious plants in the genus *Schiedea*.

## 2 Evolutionary model

### 2.1 Rates of coalescence and mutation

In large populations, switching of lineages between uniparental and biparental carriers occurs on the order of generations, virtually instantaneously relative to the rate at which lineages residing in distinct individuals coalesce (Nordborg and Donnelly, 1997; Fu, 1997). Here, we describe the structure of the coalescence process shared by our models of pure hermaphroditism, androdioecy, and gynodioecy.

**Uniparental proportion and the rate of parent-sharing:** In populations reproducing through a mixture of self-fertilization and random outcrossing, the rate of coalescence is determined by the probability that a random individual is uniparental ( $s^*$ , the uniparental proportion) and the rate at which genetic lineages sampled from distinct individuals derive from the same individual in the immediately preceding generation ( $1/N^*$ , the rate of parent-sharing).

For a given breeding system,  $s^*$  denotes the probability that a random individual is uniparental. Under pure hermaphroditism, for example,  $s^*$  corresponds to

$$s_H = \frac{\tilde{s}\tau}{\tilde{s}\tau + 1 - \tilde{s}}, \quad (1a)$$

for  $\tilde{s}$  the fraction of uniparental offspring at conception and  $\tau$  the rate of survival of uniparental relative to biparental offspring. Also under pure hermaphroditism, the probability that a pair of genes, randomly sampled from distinct individuals, derive from the same individual in the immediately preceding generation is

$$1/N_H = [s_H^2 + 4s_H(1 - s_H)(1/2) + 4(1 - s_H)^2(1/4)] / N_h = 1/N_h, \quad (1b)$$

independent of the rates of inbreeding and inbreeding depression (see Appendix A).

These expressions (1), which assume pure hermaphroditism, are equivalent to those obtained by Fu (1997) and Nordborg and Donnelly (1997). In androdioecious populations, comprising  $N_h$  reproducing hermaphrodites and  $N_m$  reproducing males (female-steriles), the uniparental proportion ( $s^*$ ) is identical to the case of pure hermaphroditism (1a)

$$s_A = \frac{\tilde{s}\tau}{\tilde{s}\tau + 1 - \tilde{s}}, \quad (2a)$$

and a pair of genes sampled from distinct individuals derive from the same parent ( $1/N^*$ ) with probability

$$\frac{1}{N_A} = \frac{(1 + s_A)^2}{4N_h} + \frac{(1 - s_A)^2}{4N_m}. \quad (2b)$$

In the absence of inbreeding ( $s_A = 0$ ), this expression reduces to the classical harmonic mean expression for effective population size (Wright, 1969). In gynodioecious populations, comprising  $N_h$  reproducing hermaphrodites and  $N_f$  reproducing females (male-steriles), the uniparental proportion ( $s^*$ ) corresponds to

$$s_G = \frac{\tau N_h a}{\tau N_h a + N_h(1 - a) + N_f \sigma}, \quad (3a)$$

in which  $\sigma$  represents the seed fertility of females relative to hermaphrodites and  $a$  the proportion of seeds of hermaphrodites set by self-pollen. The probability that a pair of genes sampled from distinct individuals derive from the same parent ( $1/N^*$ ) is

$$\frac{1}{N_G} = \frac{[2 - (1 - s_G)(1 - H)]^2}{4N_h} + \frac{[(1 - s_G)(1 - H)]^2}{4N_f}, \quad (3b)$$

in which

$$H = \frac{N_h(1 - a)}{N_h(1 - a) + N_f \sigma} \quad (4)$$

represents the proportion of biparental offspring that have a hermaphroditic seed parent. Appendix A presents full derivations of the uniparental proportion  $s^*$  and the rate of parent-sharing  $1/N^*$  under the three reproductive systems considered here.

**Relative rates of coalescence and mutation:** Fundamental to coalescence-based analyses of patterns of genetic variation is the rate of coalescence of genetic lineages, which depends on the uniparental fraction ( $s^*$ ) and the rate of parent-sharing ( $1/N^*$ ), relative to the rate of mutation.

We have determined for three iconic mating systems the rate of parent-sharing  $1/N^*$ , the probability that a pair of genes sampled from distinct individuals derive from the same individual in the immediately preceding generation. The two lineages descend from the same gene (immediate coalescence) or from distinct genes in that individual with equal probability. In the latter case, the individual is either uniparental (probability  $s^*$ ), implying descent once again of the lineages from a single individual in the preceding generation, or biparental, implying descent from distinct parents. Residence of a pair of lineages in a single individual rapidly resolves either to coalescence, with probability

$$f_c = \frac{s^*}{2 - s^*}, \quad (5)$$

or to residence in distinct individuals, with the complement probability. This expression is identical to the classical coefficient of inbreeding (Wright, 1921; Haldane, 1924). The total rate of coalescence of lineages sampled from distinct individuals corresponds to

$$\frac{(1 + f_c)/2}{N^*} = \frac{1}{N^*(2 - s^*)}. \quad (6)$$

Let  $u$  denote the rate of mutation under the infinite alleles model and  $1/N^*$  the rate at which a pair of lineages in distinct individuals derive in the immediately preceding generation

from the same individual (parent-sharing). Our model assumes that parent-sharing and mutation occur on comparable time scales:

$$\begin{aligned} \lim_{\substack{N \rightarrow \infty \\ u \rightarrow 0}} 4Nu &= \theta \\ \lim_{\substack{N \rightarrow \infty \\ N^* \rightarrow \infty}} N/N^* &= c, \end{aligned} \tag{7}$$

for  $\theta$  the scaled rate of mutation,  $c$  the scaled rate of coalescence, and  $N$  an arbitrary quantity that goes to infinity at a rate comparable to  $N^*$  and  $1/u$  (see Appendix A).

Our model assumes independence between the processes of coalescence and mutation and that these processes occur on a much longer time scale than reproduction:

$$1 - s^* \gg u, 1/N^*. \tag{8}$$

For  $m$  lineages, each residing in a distinct individual, the probability that the most recent event corresponds to mutation is

$$\lim_{N \rightarrow \infty} \frac{mu}{mu + \binom{m}{2}/[N^*(2 - s^*)]} = \frac{\theta^*}{\theta^* + m - 1},$$

in which

$$\begin{aligned} \theta^* &= \lim_{\substack{N \rightarrow \infty \\ u \rightarrow 0}} 2N^*u(2 - s^*) = \lim_{\substack{N \rightarrow \infty \\ u \rightarrow 0}} 4Nu \frac{N^*}{N}(1 - s^*/2) \\ &= \theta(1 - s^*/2)/c, \end{aligned} \tag{9}$$

for  $\theta$  and  $c$  defined in (7). This key expression for  $\theta^*$  determines the probability of the observed pattern of variation under the infinite-alleles model of mutation.

## 2.2 Likelihood

Here, we describe our use of the Ewens Sampling Formula (ESF, Ewens, 1972) to determine likelihoods based on a sample of diploid multilocus genotypes.

**Overview:** For panmictic populations, the ESF provides the probability, under the infinite-alleles model of mutation, of an allele frequency spectrum (AFS) observed at a single locus. For populations reproducing through partial-self-fertilization, the ESF under scaled mutation rate  $\theta^*$  (9) provides the probability of the AFS in a sample of genes at a given locus, each taken from a distinct individual. This rescaling of time by the rate of inbreeding (see Nordborg and Donnelly, 1997) permits estimation of composite parameter  $\theta^*$ , but not the uniparental proportion  $s^*$  apart from the scaled mutation rate. By accommodating a sample of diploid genotypes and accounting for identity disequilibrium (Cockerham and Weir, 1968), the correlation in heterozygosity across loci generated by their common recent history of inbreeding, we develop a basis for the estimation of both  $\theta^*$  and  $s^*$ . This framework also permits estimation of parameters beyond  $\theta^*$  and  $s^*$  (*e.g.*, level of inbreeding depression or seed fertility of male-sterile individuals relative to hermaphroditic individuals), but requires additional information, including for example observations of the relative proportions of female-steriles and hermaphrodites.

**Genealogical histories:** For a sample comprising up to 2 alleles at each of  $L$  autosomal loci in  $n$  diploid individuals, we represent the observed genotypes by

$$\mathbf{X} = \{\mathbf{X}_1, \mathbf{X}_2, \dots, \mathbf{X}_L\}, \quad (10)$$

in which  $\mathbf{X}_l$  denotes the set of genotypes observed at locus  $l$ ,

$$\mathbf{X}_l = \{\mathbf{X}_{l1}, \mathbf{X}_{l2}, \dots, \mathbf{X}_{ln}\}, \quad (11)$$

with

$$\mathbf{X}_{lk} = (X_{lk1}, X_{lk2})$$

the genotype at locus  $l$  of individual  $k$ , with alleles  $X_{lk1}$  and  $X_{lk2}$ .

To facilitate accounting for the shared recent history of genes borne by an individual in sample, we introduce latent variables

$$\mathbf{T} = \{T_1, T_2, \dots, T_n\}, \quad (12)$$

for  $T_k$  denoting the number of consecutive generations of selfing in the immediate ancestry of the  $k^{\text{th}}$  individual, and

$$\mathbf{I} = \{I_{lk}\}, \quad (13)$$

for  $I_{lk}$  indicating whether the lineages borne by the  $k^{\text{th}}$  individual at locus  $l$  coalesce within the most recent  $T_k$  generations. Independent of other individuals, the number of consecutive generations of inbreeding in the ancestry of the  $k^{\text{th}}$  individual is geometrically distributed:

$$T_k \sim \text{Geometric}(s^*), \quad (14)$$

with  $T_k = 0$  signifying that individual  $k$  is the product of random outcrossing. Irrespective of whether 0, 1, or 2 of the genes at locus  $l$  in individual  $k$  are observed,  $I_{lk}$  indicates whether the two genes at that locus in individual  $k$  coalesce during the  $T_k$  consecutive generations of inbreeding in its immediate ancestry:

$$I_{lk} = \begin{cases} 0 & \text{if the two genes do not coalesce} \\ 1 & \text{if the two genes coalesce.} \end{cases}$$

Because the pair of lineages at any locus coalesce with probability  $\frac{1}{2}$  in each generation of selfing,

$$\Pr(I_{lk} = 0) = \frac{1}{2^{T_k}} = 1 - \Pr(I_{lk} = 1). \quad (15)$$

Figure 1 depicts the recent genealogical history at a locus  $l$  in 5 individuals. Individuals 2 and 5 are products of random outcrossing ( $T_2 = T_5 = 0$ ), while the others derive from some positive number of consecutive generations of selfing in their immediate ancestry ( $T_1 = 2, T_3 = 3, T_4 = 1$ ). Both individuals 1 and 3 are homozygotes ( $\alpha\alpha$ ), with the lineages of individual 3 but not 1 coalescing more recently than the most recent outcrossing event ( $I_{l1} = 0, I_{l3} = 1$ ). As individual 2 is heterozygous ( $\alpha\beta$ ), its lineages necessarily remain distinct since the most recent outcrossing event ( $I_{l2} = 0$ ). One gene in each of individuals 4

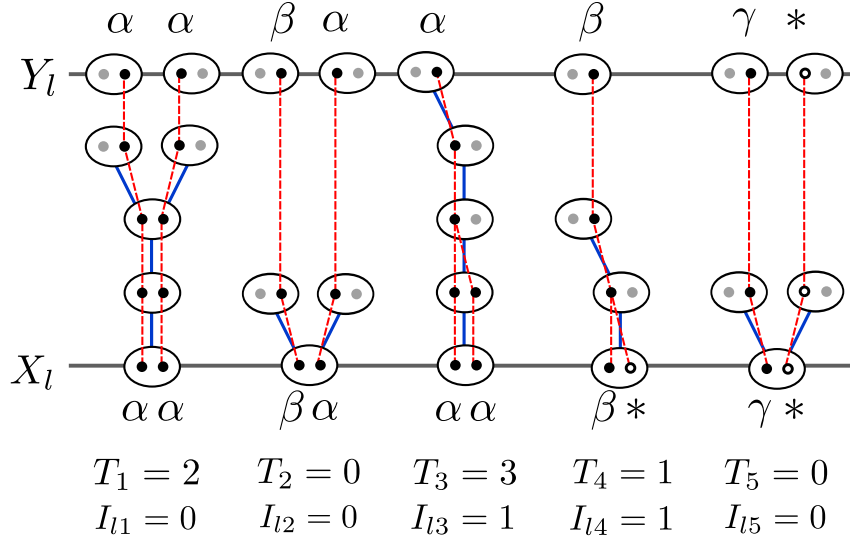


Fig. 1: Ancestry of individuals (blue) and their genes (red) back to the most recent outcrossing event. Filled dots represent sampled genes for which the allelic class is observed (Greek letters) and their ancestral lineages. Open dots represent genes in the sample with unobserved allelic class (\*). Grey dots represent other genes carried by ancestors of the sampled individuals. The relationship between the observed sample  $\mathbf{X}_l$  and the ancestral sample  $\mathbf{Y}_l$  is determined by the intervening coalescence events  $\mathbf{I}_l$ .

and 5 are unobserved (\*), with the unobserved lineage in individual 4 but not 5 coalescing more recently than the most recent outcrossing event ( $I_{l4} = 1, I_{l5} = 0$ ).

In addition to the observed sample of diploid individuals, we consider the state of the sampled lineages at the most recent generation in which an outcrossing event has occurred in the ancestry of all  $n$  individuals. This point in the history of the sample occurs  $\hat{T}$  generations into the past, for

$$\hat{T} = 1 + \max_k T_k.$$

In Fig. 1, for example,  $\hat{T} = 4$ , reflecting the most recent outcrossing event in the ancestry of individual 3. The ESF provides the probability of the allele frequency spectrum at this point.

We represent the ordered list of allelic states of the lineages at  $\hat{T}$  generations into the past by

$$\mathbf{Y} = \{\mathbf{Y}_1, \mathbf{Y}_2, \dots, \mathbf{Y}_L\}, \quad (16)$$

for  $\mathbf{Y}_l$  a list of ancestral genes in the same order as their descendants in  $\mathbf{X}_l$ . Each gene in  $\mathbf{Y}_l$  is the ancestor of either 1 or 2 genes at locus  $l$  from a particular individual in  $\mathbf{X}_l$  (11), depending on whether the lineages held by that individual coalesce during the consecutive generations of inbreeding in its immediate ancestry. We represent the number of genes in  $\mathbf{Y}_l$  by  $m_l$  ( $n \leq m_l \leq 2n$ ). In Figure 1, for example,  $\mathbf{X}_l$  contains 10 genes in 5 individuals, but  $\mathbf{Y}_l$  contains only 8 genes, with  $Y_{l1}$  the ancestor of only the first allele of  $\mathbf{X}_{l1}$  and  $Y_{l5}$  the ancestor of both alleles of  $\mathbf{X}_{l3}$ .

We assume (8) that the initial phase of consecutive generations of selfing is sufficiently short to ensure a negligible probability of mutation in any lineage at any locus and a negligible

probability of coalescence between lineages held by distinct individuals more recently than  $\hat{T}$ . Accordingly, the coalescence history  $\mathbf{I}$  (13) completely determines the correspondence between genetic lineages in  $\mathbf{X}$  (10) and  $\mathbf{Y}$  (16).

**Computing the likelihood:** In principle, the likelihood of the observed data can be computed from the augmented likelihood by summation:

$$\Pr(\mathbf{X}|\Theta^*, s^*) = \sum_{\mathbf{I}} \sum_{\mathbf{T}} \Pr(\mathbf{X}, \mathbf{I}, \mathbf{T}|\Theta^*, s^*), \quad (17)$$

for

$$\Theta^* = \{\theta_1^*, \theta_2^*, \dots, \theta_L^*\} \quad (18)$$

the list of scaled, locus-specific mutation rates,  $s^*$  the population-wide uniparental proportion for the reproductive system under consideration (*e.g.*, (1a) for the pure hermaphroditism model), and  $\mathbf{T}$  (12) and  $\mathbf{I}$  (13) the lists of latent variables representing the time since the most recent outcrossing event and whether the 2 lineages borne by a sampled individual coalesce during this period. Here we follow a common abuse of notation in using  $\Pr(\mathbf{X})$  to denote  $\Pr(\mathbf{X} = \mathbf{x})$  for random variable  $\mathbf{X}$  and realized value  $\mathbf{x}$ . Summation (17) is computationally expensive: the number of consecutive generations of inbreeding in the immediate ancestry of an individual ( $T_k$ ) has no upper limit (compare David et al., 2007) and the number of combinations of coalescence states ( $I_{lk}$ ) across the  $L$  loci and  $n$  individuals increases exponentially ( $2^{Ln}$ ) with the total number of assignments. We perform Markov chain Monte Carlo (MCMC) to avoid both these sums.

To calculate the augmented likelihood, we begin by applying Bayes rule:

$$\Pr(\mathbf{X}, \mathbf{I}, \mathbf{T}|\Theta^*, s^*) = \Pr(\mathbf{X}, \mathbf{I}|\mathbf{T}, \Theta^*, s^*) \Pr(\mathbf{T}|\Theta^*, s^*).$$

Because the times since the most recent outcrossing event  $\mathbf{T}$  depend only on the uniparental proportion  $s^*$ , through (14), and not on the rates of mutation  $\Theta^*$ ,

$$\Pr(\mathbf{T}|\Theta^*, s^*) = \prod_{k=1}^n \Pr(T_k|s^*).$$

Even though our model assumes the absence of physical linkage among any of the loci, the genetic data  $\mathbf{X}$  and coalescence events  $\mathbf{I}$  are not independent across loci because they depend on the times since the most recent outcrossing event  $\mathbf{T}$ . Given  $\mathbf{T}$ , however, the genetic data and coalescence events are independent across loci

$$\Pr(\mathbf{X}, \mathbf{I}|\mathbf{T}, \Theta^*, s^*) = \prod_{l=1}^L \Pr(\mathbf{X}_l, \mathbf{I}_l|\mathbf{T}, \theta_l^*, s^*).$$

Further,

$$\begin{aligned} \Pr(\mathbf{X}_l, \mathbf{I}_l|\mathbf{T}, \theta_l^*, s^*) &= \Pr(\mathbf{X}_l|\mathbf{I}_l, \mathbf{T}, \theta_l^*, s^*) \cdot \Pr(\mathbf{I}_l|\mathbf{T}, \theta_l^*, s^*) \\ &= \Pr(\mathbf{X}_l|\mathbf{I}_l, \theta_l^*, s^*) \cdot \prod_{k=1}^n \Pr(I_{lk}|T_k). \end{aligned}$$



This expression reflects that the times to the most recent outcrossing event  $\mathbf{T}$  affect the observed genotypes  $\mathbf{X}_l$  only through the coalescence states  $\mathbf{I}_l$  and that the coalescence states  $\mathbf{I}_l$  depend only on the times to the most recent outcrossing event  $\mathbf{T}$ , through (15).

To compute  $\Pr(\mathbf{X}_l|\mathbf{I}_l, \theta_l^*, s^*)$ , we incorporate latent variable  $\mathbf{Y}_l$  (16), describing the states of lineages at the most recent point at which all occur in distinct individuals (Fig. 1):

$$\begin{aligned} \Pr(\mathbf{X}_l|\mathbf{I}_l, \theta_l^*, s^*) &= \sum_{\mathbf{Y}_l} \Pr(\mathbf{X}_l, \mathbf{Y}_l|\mathbf{I}_l, \theta_l^*, s^*) \\ &= \sum_{\mathbf{Y}_l} \Pr(\mathbf{X}_l|\mathbf{Y}_l, \mathbf{I}_l, \theta_l^*, s^*) \Pr(\mathbf{Y}_l|\mathbf{I}_l, \theta_l^*, s^*) \\ &= \sum_{\mathbf{Y}_l} \Pr(\mathbf{X}_l|\mathbf{Y}_l, \mathbf{I}_l) \cdot \Pr(\mathbf{Y}_l|\mathbf{I}_l, \theta_l^*), \end{aligned} \quad (19a)$$

reflecting that the coalescence states  $\mathbf{I}_l$  establish the correspondence between the spectrum of genotypes in  $\mathbf{X}_l$  and the spectrum of alleles in  $\mathbf{Y}_l$  and that the distribution of  $\mathbf{Y}_l$ , given by the ESF, depends on the uniparental proportion  $s^*$  only through the scaled mutation rate  $\theta_l^*$  (9).

Given the sampled genotypes  $\mathbf{X}_l$  and coalescence states  $\mathbf{I}_l$ , at most one ordered list of alleles  $\mathbf{Y}_l$  produces positive  $\Pr(\mathbf{X}_l|\mathbf{Y}_l, \mathbf{I}_l)$  in (19a). Coalescence of the lineages at locus  $l$  in any heterozygous individual (*e.g.*,  $X_{lk} = (\beta, \alpha)$  with  $I_{lk} = 1$  in Fig. 1) implies

$$\Pr(\mathbf{X}_l|\mathbf{Y}_l, \mathbf{I}_l) = 0$$

for all  $\mathbf{Y}_l$ . Any non-zero  $\Pr(\mathbf{X}_l|\mathbf{Y}_l, \mathbf{I}_l)$  precludes coalescence in any heterozygous individual and  $\mathbf{Y}_l$  must specify the observed alleles of  $\mathbf{X}_l$  in the order of observation, with either 1 ( $I_{lk} = 1$ ) or 2 ( $I_{lk} = 0$ ) instances of the allele for any homozygous individual (*e.g.*,  $X_{lk} = (\alpha, \alpha)$ ). For all cases with non-zero  $\Pr(\mathbf{X}_l|\mathbf{Y}_l, \mathbf{I}_l)$ ,

$$\Pr(\mathbf{X}_l|\mathbf{Y}_l, \mathbf{I}_l) = 1.$$

Accordingly, expression (19a) reduces to

$$\Pr(\mathbf{X}_l|\mathbf{I}_l, \theta_l^*, s^*) = \sum_{\mathbf{Y}_l: \Pr(\mathbf{X}_l|\mathbf{Y}_l, \mathbf{I}_l) \neq 0} \Pr(\mathbf{Y}_l|\mathbf{I}_l, \theta_l^*), \quad (19b)$$

a sum with either 0 or 1 terms. Because all genes in  $\mathbf{Y}_l$  reside in distinct individuals, we obtain  $\Pr(\mathbf{Y}_l|\mathbf{I}_l, \theta_l^*)$  from the Ewens Sampling Formula for a sample, of size

$$m_l = 2n - \sum_{k=1}^n I_{lk},$$

ordered in the sequence in which the genes are observed.

A well-known property of the ESF (Ewens, 1972; Karlin and McGregor, 1972) is that given the spectrum of alleles observed among  $i - 1$  genes, the probability that the next-sampled ( $i^{\text{th}}$ ) gene represents a novel allele corresponds to

$$\pi_i = \frac{\theta^*}{i - 1 + \theta^*}, \quad (20)$$

for  $\theta^*$  defined in (9), and the probability that it represents an additional copy of allele  $j$  is

$$(1 - \pi_i) \frac{i_j}{i - 1},$$

for  $i_j$  the number of replicates of allele  $j$  already observed ( $\sum_j i_j = i - 1$ ). These expressions provide  $\Pr(\mathbf{Y}_l | \mathbf{I}_l, \theta_l^*)$  in (19b). Explicitly, for  $\mathbf{Y}_l$  the ordered list of alleles observed in the sample at locus  $l$ ,

$$\Pr(\mathbf{Y}_l | \mathbf{I}_l, \theta_l^*) = \frac{(\theta_l^*)^{K_l} \prod_{j=1}^{K_l} (m_{lj} - 1)!}{\prod_{i=1}^{m_l} (i - 1 + \theta_l^*)}, \quad (21)$$

in which  $K_l$  denotes the total number of distinct allelic classes,  $m_{lj}$  the number of replicates of the  $j^{\text{th}}$  allele in the sample, and  $m_l = \sum_j m_{lj}$  the number of lineages remaining at time  $\hat{T}$  (Fig. 1).

**Missing data:** Our method allows the allelic class of one or both genes at each locus to be missing. In Fig. 1, for example, the genotype of individual 4 is  $\mathbf{X}_{l4} = (\beta, *)$ , indicating that the allelic class of the first gene is observed to be  $\beta$ , but that of the second gene is unknown.

A missing allelic specification in the sample of genotypes  $\mathbf{X}_l$  leads to a missing specification for the corresponding gene in  $\mathbf{Y}_l$  unless the genetic lineage coalesces with a lineage with an observed allele in the period between  $\mathbf{X}_l$  and  $\mathbf{Y}_l$ . Figure 1 illustrates such a coalescence event in the case of individual 4. In contrast, the lineages ancestral to the genes carried by individual 5 fail to coalesce more recently than their separation into distinct individuals, giving rise to a missing specification in  $\mathbf{Y}_l$ .

The probability of  $\mathbf{Y}_l$  can be computed by simply summing over all possible values for each missing specification. Equivalently, those elements may simply be dropped from  $\mathbf{Y}_l$  before computing the probability via the ESF, the procedure implemented in our method.

### 3 Bayesian inference framework

Derivations presented in the preceding section indicate that the probability of a sample of diploid genotypes under the infinite alleles model depends on only the uniparental proportion  $s^*$  and the scaled mutation rates  $\Theta^*$  (18) across loci, composite parameters that are functions of the basic demographic parameters characterizing each model of reproduction under consideration (Appendix A). As a consequence, the genotypic data provide equal support to any combination of basic parameters that implies the same values of  $s^*$  and  $\Theta^*$ .

Although some basic parameters of a given model may be unidentifiable from the genotypic data alone, our MCMC implementation updates the basic parameters directly, with likelihoods determined from the implied values of  $s^*$  and  $\Theta^*$ . This feature facilitates the incorporation of information in addition to the genotypic data that can contribute to the estimation of the basic parameters under a particular model or assessment of alternative models.

### 3.1 Prior on mutation rates

Ewens (1972) showed for the panmictic case that the number of distinct allelic classes observed at a locus (*e.g.*,  $K_l$  in (21)) provides a sufficient statistic for the estimation of the scaled mutation rate. Because each locus  $l$  provides relatively little information about the scaled mutation rate  $\theta_l^*$  (9), we assume that mutation rates across loci cluster in a finite number of groups. However, we do not know *a priori* the group assignment of loci or even the number of distinct rate classes among the observed loci. We make use of the Dirichlet process prior to estimate simultaneously the number of groups, the value of  $\theta^*$  for each group, and the assignment of loci to groups.

The Dirichlet process comprises a base distribution, which here represents the distribution of the scaled mutation rate  $\theta^*$  across groups, and a concentration parameter  $\alpha$ , which controls the probability that each successive locus forms a new group. We assign 0.1 to  $\alpha$  of the Dirichlet process, and place a gamma distribution ( $\Gamma(\alpha = 0.25, \beta = 2)$ ) on the mean scaled mutation rate for each group. As this prior has a high variance relative to the mean (0.5), it is relatively uninformative about  $\theta^*$ .

### 3.2 Models of reproduction

In addition to the scaled mutation rates  $\Theta^*$  (18) across loci, each of the pure hermaphroditism, androdioecy, and gynodioecy models addressed here comprise a set of demographic parameters  $\Psi$  (Appendix A). We have

$$\begin{aligned} \Pr(\mathbf{X}, \Theta^*, \Psi) &= \Pr(\mathbf{X}|\Theta^*, \Psi) \cdot \Pr(\Theta^*) \cdot \Pr(\Psi) \\ &= \Pr(\mathbf{X}|\Theta^*, s^*(\Psi)) \cdot \Pr(\Theta^*) \cdot \Pr(\Psi), \end{aligned}$$

for  $\mathbf{X}$  the genotypic data and  $s^*(\Psi)$  the uniparental fraction determined by  $\Psi$  for the model under consideration. To determine  $\theta_l$  (7) for each locus  $l$ , we solve (9), using  $s^*(\Psi)$  and  $c(\Psi)$ , the scaling factor defined in (7).

**Pure hermaphroditism:** Beyond the scaled mutation rates  $\Theta^*$  (9), this model comprises the single parameter  $s^*$ , which is itself a function of the proportion of conceptions through selfing  $\tilde{s}$  and the relative viability of uniparental offspring  $\tau$  (Appendix A). We assume a uniform prior for  $s^*$ :

$$s^* \sim \text{Uniform}(0, 1).$$

**Androdioecy:** For this model,  $\Psi = \{\tilde{s}, \tau, \rho_m\}$ , for  $\rho_m$  (A.2) the proportion of males among reproductives. We again assume uniform priors:

$$\begin{aligned} s^* &\sim \text{Uniform}(0, 1) \\ \rho_m &\sim \text{Uniform}(0, 1). \end{aligned}$$

Additional data are required to make these parameters identifiable. For example, counts of the number of males ( $C_m$ ) among the  $n$  sampled zygotes may be incorporated into the likelihood:

$$\Pr(\mathbf{X}, \mathbf{I}, \mathbf{T}, C_m | s^*, \rho_m, \Theta^*) = \Pr(\mathbf{X}, \mathbf{I}, \mathbf{T} | s^*, \Theta^*) \cdot \Pr(C_m | \rho_m),$$

for

$$\Pr(C_m | \rho_m) \sim \text{Binomial}(n, \rho_m).$$

The ability to do inference on parameters unidentifiable from the genotypic data  $\mathbf{X}$  alone opens exciting new possibilities for inference. For example, given genetic data that are informative about  $s^*$ , data on  $\tilde{s}$  would allow for the inference of the inbreeding depression  $\tau$ . Similarly, information on the degree of inbreeding depression would then allow for inference of the fraction of eggs that are self-fertilized. Such approaches are possible because our inference procedure is model-based and relies on a likelihood.

**Gynodioecy:** For this model,  $\Psi = \{a, \tau, \rho_f, \sigma\}$ , including  $a$  the proportion of conceptions by hermaphrodites through selfing,  $\rho_f$  (A.4) the proportion of females (male-steriles) among reproductives, and  $\sigma$  the fertility of male-steriles relative to hermaphrodites (Appendix A). We set the priors

$$\begin{aligned} a &\sim \text{uniform}(0, 1) \\ \rho_f &\sim \text{uniform}(0, 1), \end{aligned}$$

but use this model to illustrate the incorporation of additional data on inbreeding depression ( $\tau$ ). While a full treatment of data from greenhouse experiments informative about  $\tau$  would require the development of a likelihood function that explicitly models the results of those experiments, we here incorporate results reported by Sakai et al. (1989) through a prior distribution:

$$\tau \sim \text{Beta}(2, 8).$$

Additional data on the female fraction ( $\rho_f$ ), for example, would enhance identifiability and improve the estimation of all parameters.

## 4 Results

### 4.1 Accuracy and coverage from simulated data

To assess the accuracy and coverage properties of our method and other methods, we developed a forward-in-time simulator of a pure-hermaphrodite population under the Wright-Fisher model of genetic drift and applied the methods to data generated by the simulator under assigned values for effective population size ( $N$ ), uniparental proportion ( $s^*$ ), and the locus-specific scaled mutation rates ( $\Theta$ ).

We compare our method to RMES (David et al., 2007) and also to estimation based simply on the observed deficiencies in heterozygotes relative to Hardy-Weinberg proportions. Under the latter approach, which we call the  $F_{IS}$  method, we estimate  $s^*$  by setting the observed value of  $F_{IS}$  equal to its classical expectation  $s^*/(2 - s^*)$  (Wright, 1921; Haldane, 1924) and solving for  $s^*$ :

$$\hat{s}^* = \frac{2\widehat{F}_{IS}}{1 + \widehat{F}_{IS}}. \quad (22)$$

### 4.1.1 Simulated data sets

Our simulator (<https://github.com/skumagai/selfingsim>) was developed using `simuPOP`, publicly available at <http://simupop.sourceforge.net/>. It explicitly represents  $N = 10,000$  individuals, each bearing two genes at each of  $L$  unlinked loci. Mutations arise at locus  $l$  at rate scaled rate  $\theta_l$  (7), in accordance with the infinite-alleles model.

We assigned values for  $s^*$  ranging from 0.01 to 0.99, with half of the  $L$  loci assigned scaled mutation rate  $\theta = 0.5$  and the remaining loci  $\theta = 1.5$ . We generated simulated data under two sampling regimes: large (sample size  $n = 70$  and  $L = 32$  loci) and small (sample size  $n = 10$  and  $L = 6$  loci).

We initialized each run with each of the  $2NL$  genes representing a distinct allele. Most of this initial heterozygosity was lost very rapidly, with the allele number and their frequency spectrum typically stabilizing within  $10N$  generations. After  $20N$  generations, we recorded the realized population and extracted a number of independent samples of size  $n$ .

Our accuracy and coverage analysis is based on  $10^2$  samples derived from each of  $10^2$  independent simulations for each set of assigned parameters.

### 4.1.2 Accuracy

We compare the bias and error of estimates of the uniparental proportion  $s^*$  obtained from `RMES` (David et al., 2007), the  $F_{IS}$  method (22), and our method. As our method is Bayesian, it generates a posterior distribution, rather than a point estimate; however, for the purposes of comparison with the point estimates of the other methods, we represent our estimate as the median of a posterior distribution.

For each method, we determine the bias and root-mean-squared error by averaging over data sets generated under each assigned value of  $s^*$ . Figure 2 indicates that the error for `RMES` exceeds the error for our method under both sampling regimes, except in cases in which the true  $s^*$  is very close to 0. For the  $n = 10$ ,  $L = 6$  sampling regime, the error of `RMES` is nearly double that of our method, whereas for the  $n = 70$ ,  $L = 32$  sampling regime, it exceeds the error for our method only slightly. The error for `RMES` rises substantially for high values of  $s^*$  under both regimes, where the error for the other two methods begins to decline. For the  $n = 70$ ,  $L = 32$  sampling regime, the `RMES` error rises steeply around  $s = 0.97$ . For the  $n = 10$ ,  $L = 6$  sampling regime, the error begins to increase more steeply at about  $s = 0.7$ . The error for the  $F_{IS}$  method also exceeds the error for our method. However, the error for the  $F_{IS}$  method is largest near  $s^* = 0$  and vanishes as  $s^*$  approaches 1.

Both `RMES` and our method have a bias that is positive near  $s^* = 0$ , but negative near  $s^* = 1$ . This is a direct result of the fact that both methods yield estimates of  $s^*$  that are constrained to lie in the interval between 0 and 1. These methods never underestimate  $s^*$  when  $s^* = 0$  and never overestimate  $s^*$  when  $s^* = 1$ . Therefore, any error near these values is unidirectional and is counted as bias. In contrast, the  $F_{IS}$  method always achieves negative bias, even near  $s^* = 0$ . This is possible because the  $F_{IS}$  method can produce negative estimates of  $s^*$ . Our method has a bias near 0 that is substantially larger than the bias of `RMES`, and an error that is slightly larger. This results from the fact that the method is Bayesian and that we report the posterior median instead of the posterior mode. The posterior distribution for  $s^*$  tends to peak at 0 (Figure 3), but the posterior median will

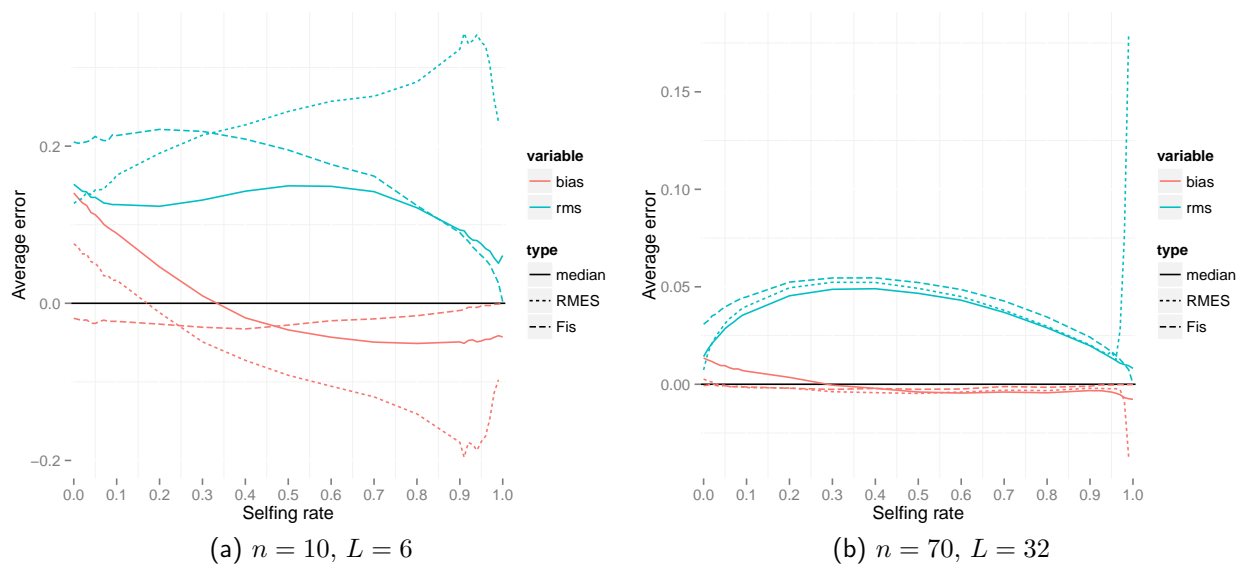


Fig. 2: Errors for the full likelihood (posterior median), RMES, and  $F_{IS}$  methods. In the legend, rms indicates the root-mean-squared error and bias the average deviation. Averages are taken across simulated data sets at each true value of  $s^*$ .

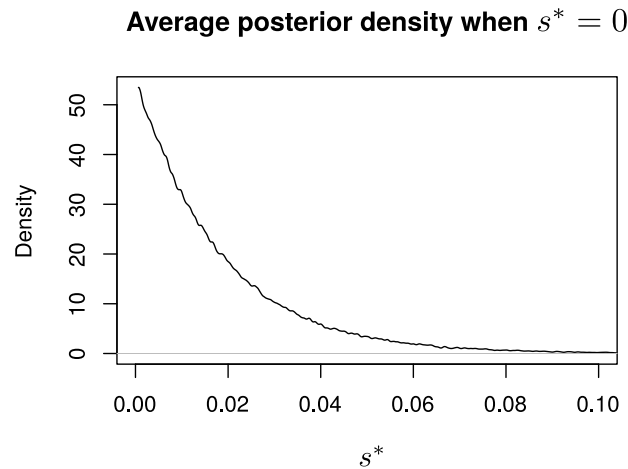


Fig. 3: for  $n = 70, L = 32$  sampling regime when  $s^* = 0$ . The average was taken across posterior densities for 100 data sets.

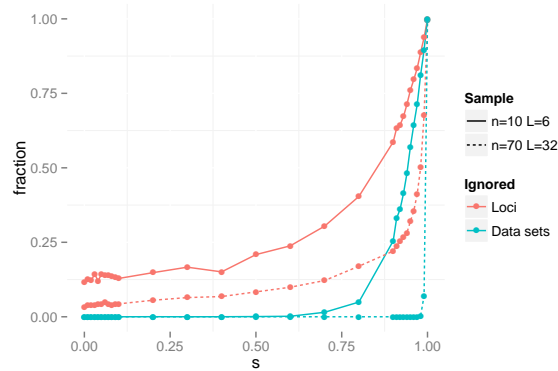


Fig. 4: Fraction of loci and data sets that are ignored by RMES.

still be greater than 0 as long as the posterior distribution contains uncertainty about the value of  $s^*$ . Since uncertainty in  $s$  never includes negative values of  $s^*$  or values greater than 1, uncertainty in  $s^*$  will be skewed upwards near  $s^* = 0$  and downwards near  $s^* = 1$ . The posterior mode does not display this large bias (Figure 20), and so we conclude that the bias merely indicates uncertainty in the posterior distribution about the value of  $s^*$  and not any preference for incorrect values.

We note that our method infers the uniparental fraction  $s^*$  under the assumption that the data were derived from a population reproducing through a mixture of self-fertilization and random outcrossing. Assessment of a model of complete random mating ( $s^* = 0$ ) against the present model ( $s^* > 0$ ) might be conducted through the Bayes factor.

In order to explain RMES's increased error at high values of  $s^*$ , we first note that the RMES software saves computation time by making the assumption that the number of selfing generations remains  $< 20$ . As  $s^*$  increases past 0.9, this becomes increasingly inaccurate, which might lead to underestimation of  $s^*$ . Additionally, RMES discards loci at which heterozygotes are not observed. Such loci are estimated by RMES to have no allelic variation in the entire population. The loci therefore become uninformative about  $s^*$ . In addition, the RMES software will not analyze data sets where less than 2 loci remain. In contrast, using the full likelihood (with alleles) makes full use of loci without heterozygotes. Such loci can constitute some of the strongest evidence toward high selfing rates, since heterozygosity has been completely eliminated. Under the  $n = 70$ ,  $L = 32$  sampling regime, 50% of loci are discarded on average when  $s^* \geq 0.94$ , but more than 90% of data sets remain analyzable even at  $s^* = 0.99$  (Figure 4). Under the  $n = 10$ ,  $L = 6$  regime, 50% of loci are discarded when  $s^*$  is greater than about 0.85, and 50% of data sets are unanalyzable when  $s^* \geq 0.94$ .

### 4.1.3 Coverage

We seek to determine if CIs computed by RMES and BCIs computed by our method have the correct properties to be considered as confidence intervals or Bayesian credible intervals. The  $F_{IS}$  method does not yield any such intervals and so we do not consider it here. For each true value of  $s^*$ , we compute the fraction of data sets where the computed interval contains the truth. This measure of coverage is a frequentist measure, since it treats each true value

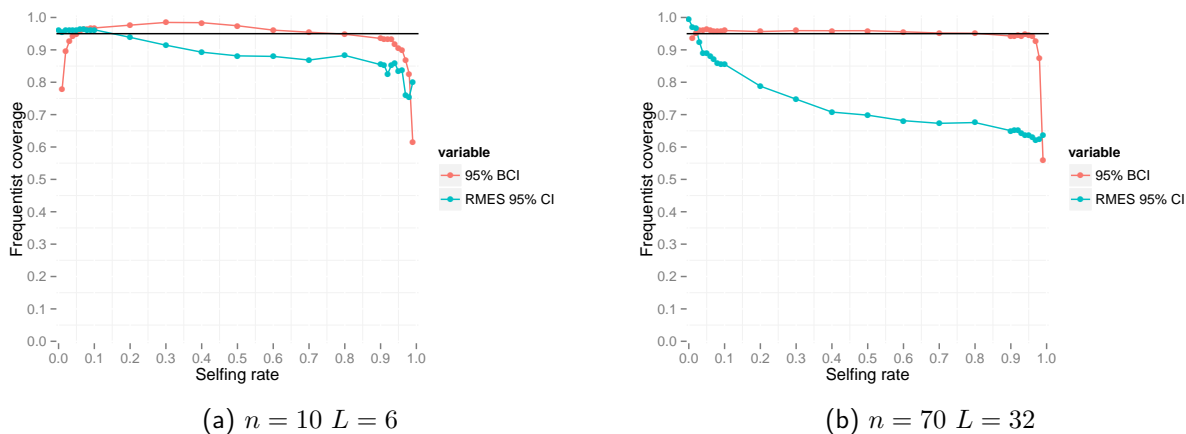


Fig. 5: Frequentist coverage at each level of  $s^*$  for 95% intervals from RMES and the method based on the full likelihood. RMES intervals are 95% confidence intervals computed via profile likelihood. Full likelihood intervals are 95% HPD Bayesian credible intervals.

of  $s^*$  separately. A 95% CI should contain the truth 95% of the time for each specific value of  $s^*$ . A 95% BCI is not expected to have 95% coverage at each value of  $s^*$ , but is expected to have 95% coverage when averaging over values of  $s^*$  sampled from the prior. We also note that there are many different BCIs for a given posterior distribution. We choose to report the highest posterior density BCI, instead of the central BCI.

Figure 5 shows that for values of  $s^*$  that are not right next to the boundaries of 0 and 1, the 95% BCIs have nearly 95% frequentist coverage for each value of  $s^*$ . These coverage properties are more exact for the  $n = 70 \ L = 32$  samples than for the  $n = 10 \ L = 6$  samples. In contrast, the RMES 95% CIs have coverage that is consistently lower than 95%. This is most pronounced for the  $n = 70 \ L = 32$  samples, where coverage that drops from 86% when  $s = 0.1$  to 64% when  $s^* = 0.99$ . Figure 6 shows that Bayesian 0.5, 0.75, 0.9, 0.95, and 0.99 credible intervals for  $s^*$  display the same pattern, with coverage being more exact for the  $n = 70 \ L = 32$  samples than for the  $n = 10 \ L = 6$  samples. For each level of credibility, coverage exceeds the desired value for intermediate values of  $s^*$ , and dips slightly below the desired value for very high and very low values of  $s^*$ . Coverage properties are also more exact for the 0.99 and 0.95 levels than for the 0.5 level.

#### 4.1.4 Distribution of selfing generations

In order to check the accuracy of our reconstructed generations of selfing, we examine the posterior distributions of selfing times  $\{T_k\}$  for  $s^* = 0.5$  under the  $n = 70, L = 32$  sampling conditions. We average posterior distributions for selfing times across 100 simulated data sets, and across individuals  $k = 1 \dots 70$  within each simulated data set. We then compare these averages based on the simulated data with the exact distribution of selfing times across individuals (Figure 7). The pooled posterior distribution closely matches the exact distribution. This simple check suggests that our method correctly infers the true posterior distribution of selfing times for each sampled individual.



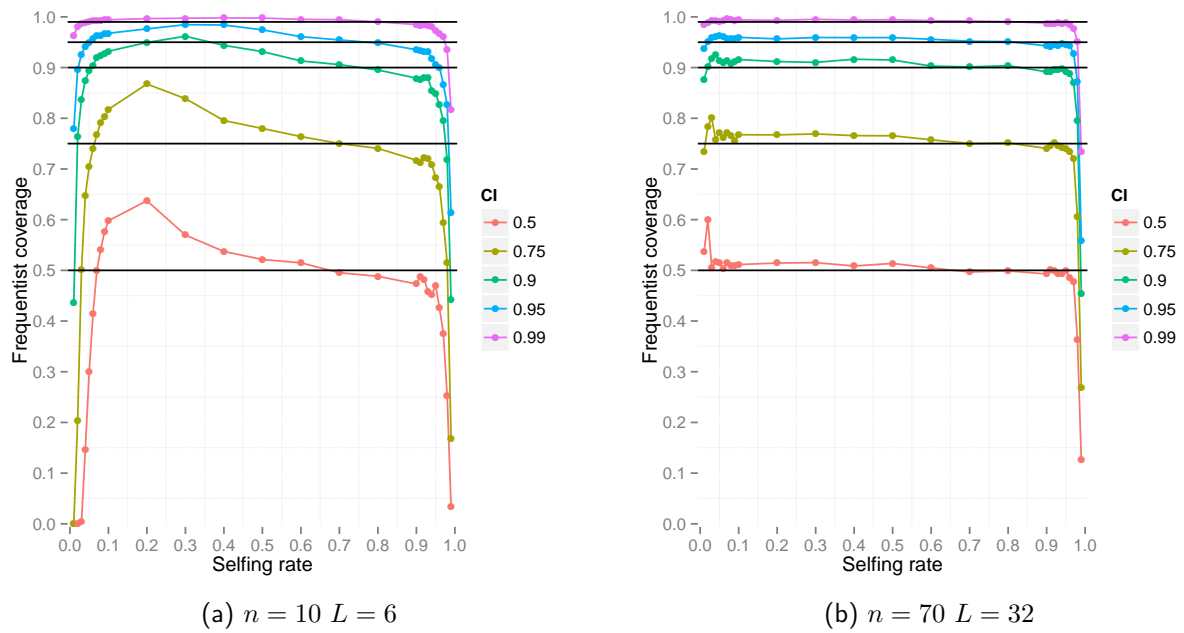


Fig. 6: Frequentist coverage for Bayesian credible intervals at different levels of credibility.

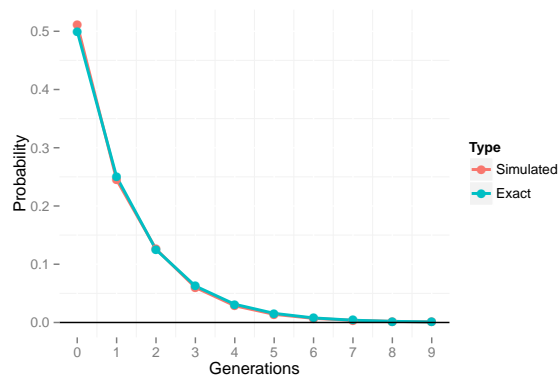


Fig. 7: times under  $s^* = 0.5$  compared to the posterior distribution averaged across individuals and across data sets.

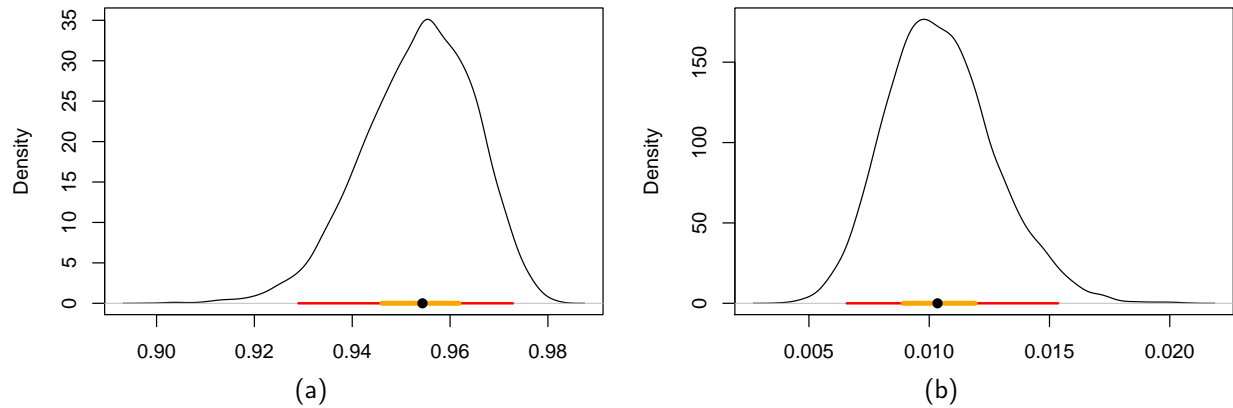


Fig. 8: Posterior distributions on (a)  $s^*$  and (b)  $\rho_m$  for the BP population. Also shown are 95% BCI (red), 50% BCI (orange), and median (black dot).

## 4.2 Androdioecy Data Example

We begin by examining data from *Kryptolebias marmoratus*, a mangrove killifish found from Florida to Brazil. *K. marmoratus* is an androdioecious fish, with rates of selfing varying between populations. We examine samples from two populations, both of which were typed at 32 microsatellite loci. We make use of the androdioecious model, incorporating data on the number of observed males for each population. If we observe  $n_m$  males out of  $n_{total}$  fish, then we incorporate such information into the likelihood by assuming

$$n_m \sim \text{Binomial}(n_{total}, p_m),$$

and multiplying the likelihood for the genetic data by  $\Pr(n_m | n_{total}, p_m)$ .

### 4.2.1 Population 1 (BP)

For the BP population we have data from 70 individuals. No males were observed in this population, so we assume that the BP population is typical of other populations with few males. We then have observations of about 20 males in about 2000 individuals across all such populations.

Estimates of the locus-specific mutation rates indicate a substantial difference in mutation rates between loci, ranging from about 0.5 to about 5 (Figure 9). The selfing rate  $s^*$  has a posterior median of 0.95 and a 95% Bayesian Credible Interval (BCI) of (0.93, 0.97) (Figure 8a). This estimate is somewhat lower than the  $F_{IS}$  estimate of 0.97. It is slightly higher than the RMES estimate of 0.94, with a 95% CI of (0.91, 0.96). We note that RMES discarded 9 out of 32 loci as useless, of which 7 were polymorphic in the sample.

The fraction of males  $p_m$  has a posterior median of 0.01 with a 95% BCI of (0.0062, 0.015) (Figure 8b). We also estimate the posterior distribution of selfing times for each individual, and display them in Figure 10. Figure 11 shows the empirical distribution of the selfing time  $T$  across individuals, averaged over posterior uncertainty.

These figures indicate a complete absence of individuals predicted to have 0 generations of selfing. This indicates that individuals with 0 generations of selfing (i.e. out-crossed

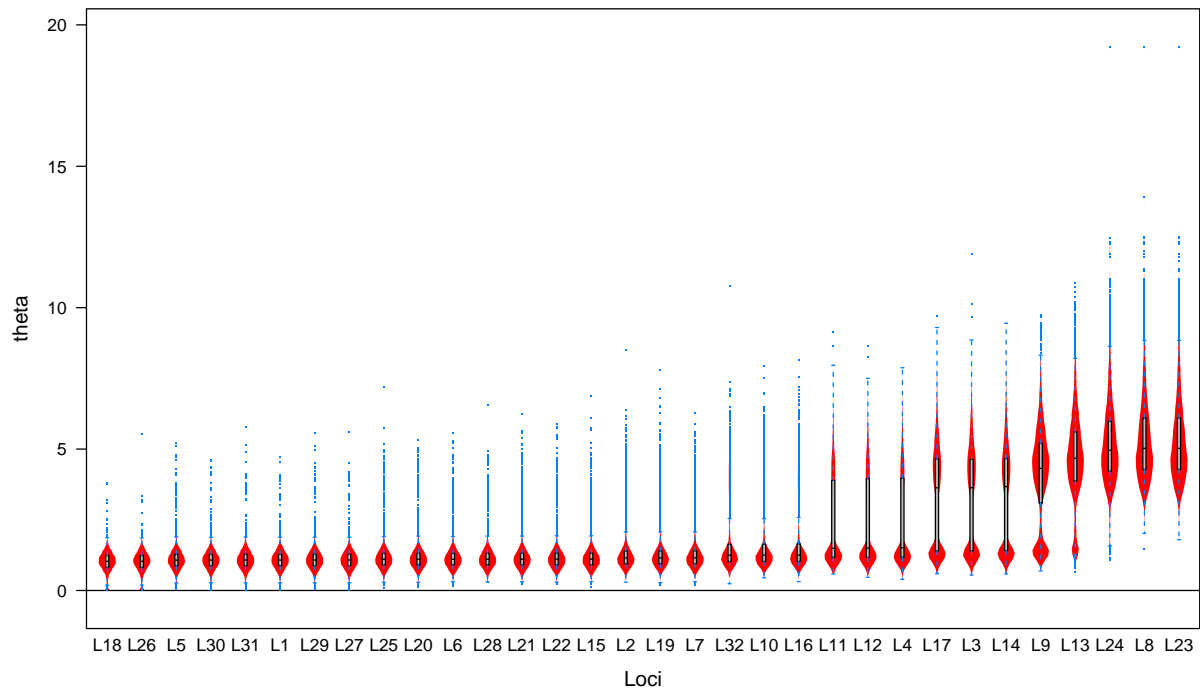


Fig. 9: Mutation rates at each locus for *K. marmoratus* (BP population). Boxes represent 50% credible intervals and lines above and below boxes represent 95% credible intervals. Posterior medians are represented by thick horizontal lines within the boxes.

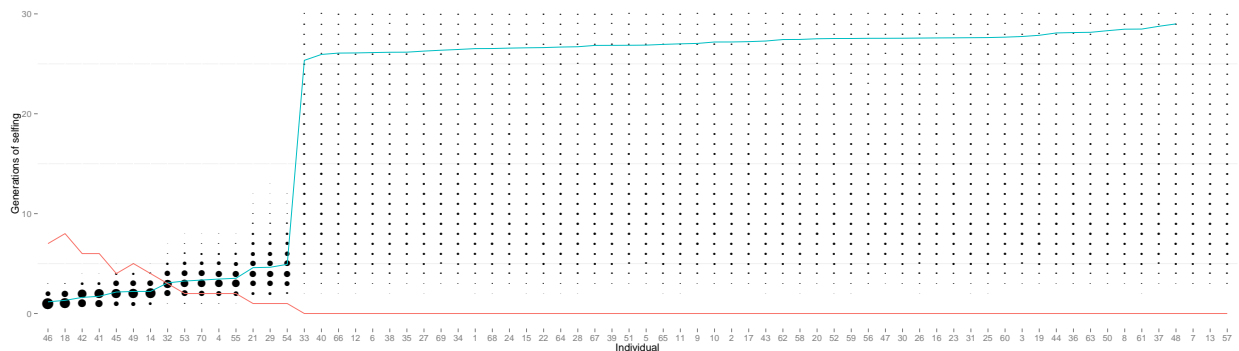


Fig. 10: Estimated number of selfing generations for each individual for *K. marmoratus* (BP population). Each dot indicates the posterior probability that a numbered individual (x-axis) has been selfed for a given number of generations (y-axis). The area of the dot is proportional to its posterior probability. Therefore the area of dots above a numbered individual sum to 1. For each individual the blue line indicates the posterior mean number of selfing generations and the red line indicates the number of heterozygous loci. The y-axis is truncated to  $[0, 30]$ .

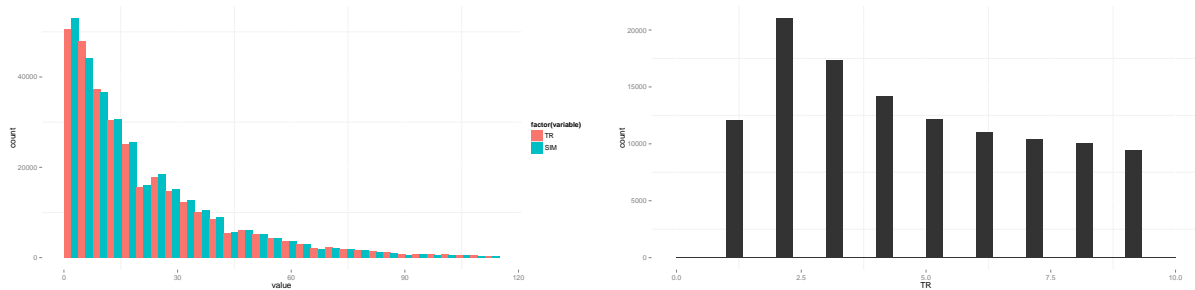


Fig. 11: Empirical distribution of selfing times  $T$  across individuals, for *K. marmoratus* (Population BP). The histogram is averaged across posterior samples. The right panel is constructed by zooming in on the panel on the left. The first bar with positive probability is for  $T = 1$ .

individuals) have less heterozygosity than predicted in a model based on selfing and panmixia alone. Out-crossed individuals thus are estimated to have undergone 1 or 2 generations of selfing. This lack of heterozygosity even among out-bred individuals suggests that population subdivision or bi-parental inbreeding may be responsible.

#### 4.2.2 Population 2 (PG)

For the PG population we have data from 59 individuals. We also have observations of 19 males out of 112 total individuals. Estimates of the mutation rates at each locus are depicted in figure 12 ; they range from about 0.5 to about 23. The selfing rate  $s^*$  has a median and 95% BCI of 0.35 (0.25, 0.45) (Figure 13a). This estimate is somewhat lower than the  $F_{IS}$  estimate of 0.39. It is slightly higher than the RMES estimate of 0.33 with a 95% CI of (0.30, 0.36). RMES discarded only 1 locus as useless here, and that locus was monomorphic in the sample.

The fraction of males  $p_m$  has a posterior median of 0.17 with a 95% BCI of (0.11, 0.25) (Figure 13b). The posterior distribution of selfing times for each individual is depicted in figure 14 . Figure shows the empirical distribution of the selfing time  $T$  across individuals, averaged over posterior uncertainty. In contrast to the previous population, this population does not seem to have significant sources of inbreeding that are not explained by selfing.

### 4.3 Gynodioecy data example

We next examine data from *Schiedea salicaria*, a gynodioecious plant in the pink family that is endemic to Hawaii. For this population, we have data on 25 individuals at 9 microsatellite loci. We also have observations of 27 females out of 221 plants. We additionally place an informative prior on the inbreeding depression  $\tau$  based on data from greenhouse experiments from Sakai et al. (1989):

$$\tau \sim \text{Beta}(2, 8).$$

Estimates of the locus-specific mutation rate do not indicate substantial evidence for differences in mutation rate across loci, with posterior medians close to 1 for all loci (Figure

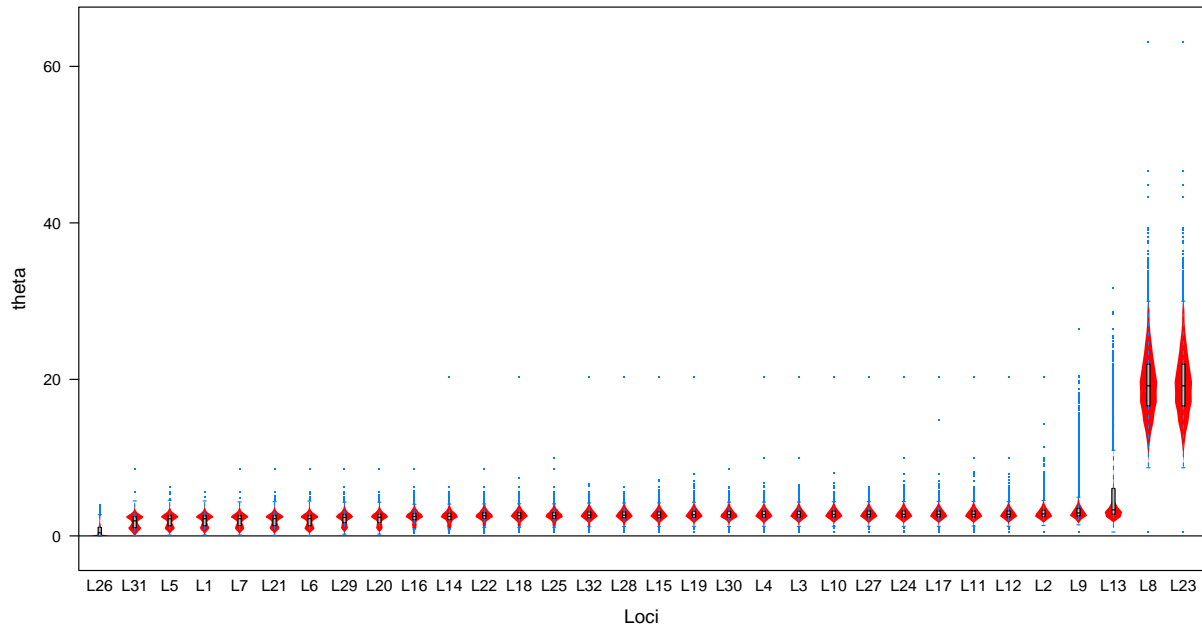


Fig. 12: Mutation rates at each locus for *K. marmoratus* (PG population).

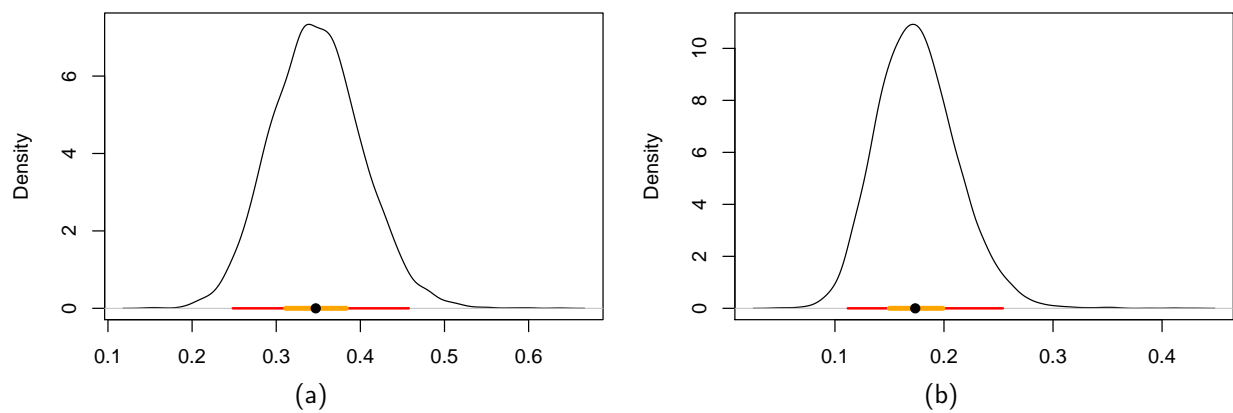


Fig. 13: Posterior distributions on (a)  $s^*$  and (b)  $\rho_m$  for the BP population. Also shown are 95% BCI (red), 50% BCI (orange), and median (black dot).

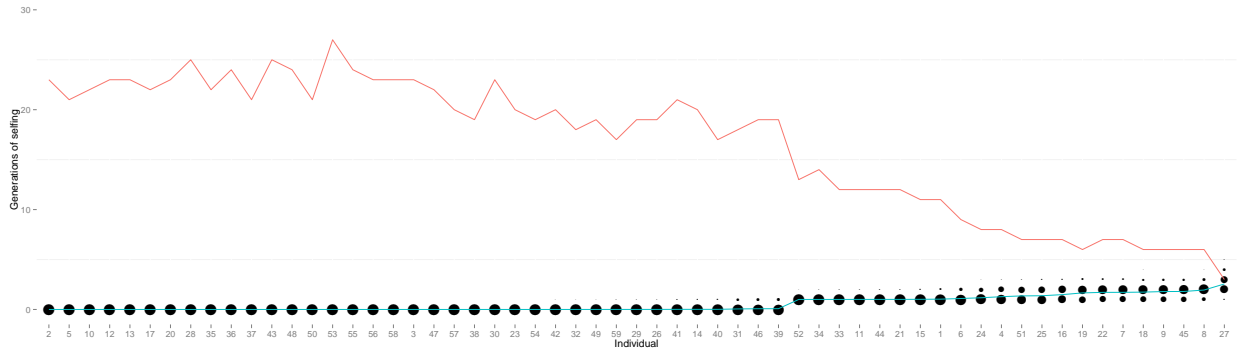


Fig. 14: Estimated number of selfing generations for each individual for *K. marmoratus* (PG population). Each dot indicates the posterior probability that a numbered individual (x-axis) has been selfed for a given number of generations (y-axis). The area of the dot is proportional to its posterior probability. Therefore the area of dots above a numbered individual sum to 1. For each individual the blue line indicates the posterior mean number of selfing generations and the red line indicates the number of heterozygous loci.

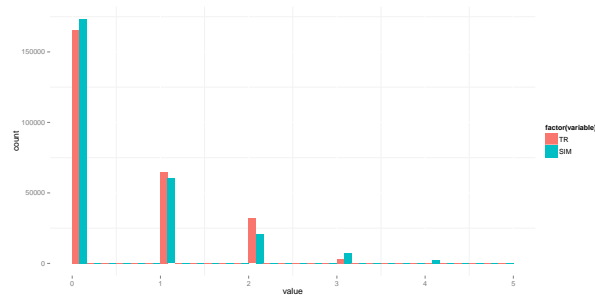


Fig. 15: Empirical distribution of selfing times  $T$  across individuals, for *K. marmoratus* (Population PG). The histogram is averaged across posterior samples.

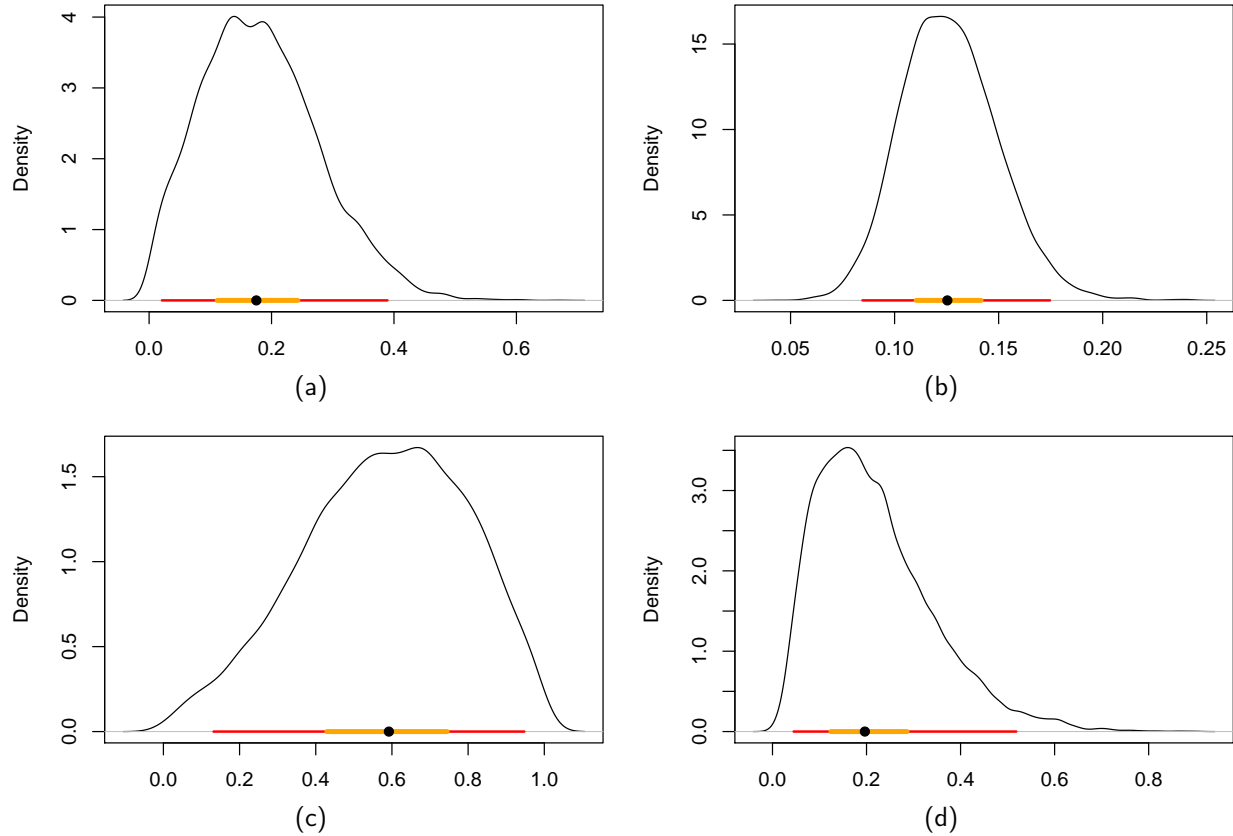


Fig. 16: Posterior distributions on (a)  $s^*$ , (b)  $\rho_f$ , (c)  $a$ , and (d)  $\tau$  for *Schiedea salicaria*. Also shown are 95% BCI (red), 50% BCI (orange), and median (black dot).

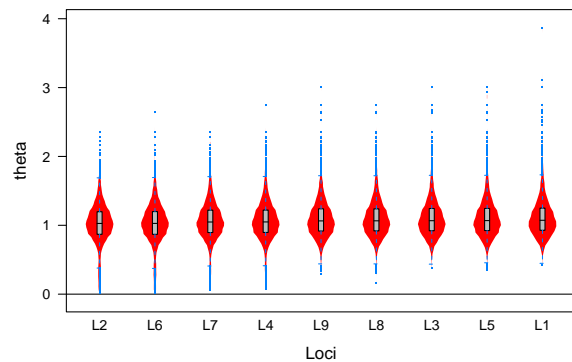


Fig. 17: Mutation rates at each locus for *S. salicaria*. Boxes represent 50% credible intervals and lines above and below boxes represent 95% credible intervals. Posterior medians are represented by thick horizontal lines within the boxes.

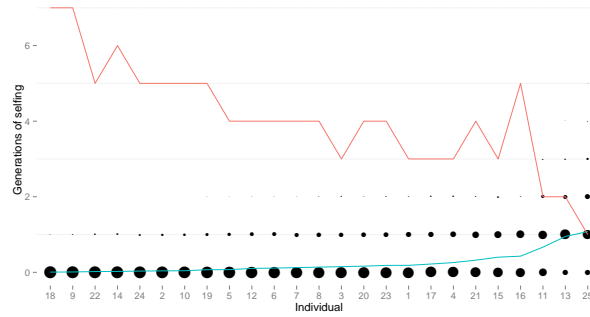


Fig. 18: Estimated number of selfing generations for each individual for *S. salicaria*. Each dot indicates the posterior probability that a numbered individual (x-axis) has been selfed for a given number of generations (y-axis). The area of the dot is proportional to its posterior probability. Therefore the area of dots above a numbered individual sum to 1. For each individual the blue line indicates the posterior mean number of selfing generations and the red line indicates the number of heterozygous loci.

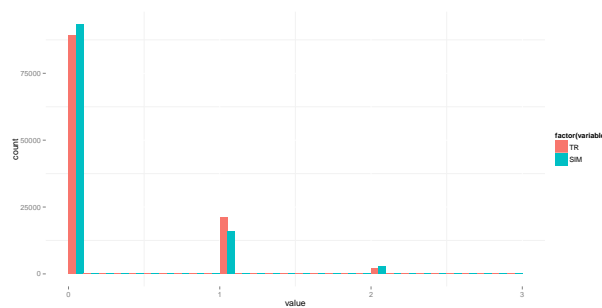


Fig. 19: Empirical distribution of selfing times  $T$  across individuals, for *S. salicaria*. The histogram is averaged across posterior samples.

17). The fraction of selfed seeds  $a$  has a posterior median of 0.612 and a 95% BCI of (0.133, 0.945). The selfing rate  $s^*$  has a posterior median of 0.17 and a 95% BCI of (.02, 0.39). This is substantially lower than the  $F_{IS}$  method's estimate of  $s^* = 0.33$ . RMES, on the other hand, gives an estimate of 0, with a 95% CI of (0, 0.15). No loci were excluded by RMES. We also estimate the selfing times for each individual, and display them in figure 18. Figure 19 shows the empirical distribution of the selfing time  $T$  across individuals, averaged over posterior uncertainty.

Posterior medians and 95% BCIs for  $a$ ,  $s^*$ ,  $\tau$ , and  $p_f$  are given in Table 1 (Figure 16). The bottom row of the table gives results for an analysis without genetic data, and with an uninformative prior on  $\tau$ . This shows that the induced prior distribution on  $s^*$  is not uniform, since the prior estimate for  $s$  is 0.0825 (0.000769, 0.656). Thus, the posterior estimate of 0.174 (0.0226, 0.380) is a substantial shift. The row second from the bottom includes no genetic data, but has an informative prior on  $\tau$ . This shifts the prior median for  $s$  down to 0.0356. Thus, the genetic data shift the posterior median of  $s$  from 0.0356 to 0.174.



Tab. 1: Parameter estimates for different amounts of data. Estimates are given by a posterior median and a 95% BCI.

Data	$a$	$s^*$	$\tau$	
genetic data + $\tau$ belief	0.612 (0.133, 0.945)	0.174 (0.0226, 0.380)	0.187 (0.0432, 0.472)	0.125 (0.000476, 0.449)
genetic data	0.646 (0.122, 0.98)	0.128 (0.00498, 0.33)	0.221 (0.0543, 0.513)	0.335 (0.028, 0.489)
$\tau$ belief	0.499 (0.0246, 0.975)	0.0356 (0.000476, 0.449)	0.18 (0.028, 0.489)	0.496 (0.0252, 0.975)
no data	0.5 (0.0251, 0.974)	0.0825 (0.000769, 0.656)	0.499 (0.0252, 0.975)	0.496 (0.0252, 0.975)

## 5 Discussion

We introduce a model-based Bayesian method for the inference of rates of self-fertilization and other aspects of a mixed mating system. Designed for genomic data, it uses the Ewens Sampling Formula (ESF) to determine likelihoods in a computationally efficient manner from frequency spectra of genotypes observed at multiple unlinked sites throughout the genome. Tests using simulated data suggest that the method provides both accurate estimates of selfing rates and accurate assessments of uncertainty.

### 5.1 A new approach to the determination of likelihoods

Enjalbert and David (2000) and David et al. (2007) base estimates of selfing rate on the distribution of numbers of heterozygous loci. Both methods strip genotype information from the data, coding any homozygote as 0 and any heterozygote as 1, irrespective of the alleles involved. Loci lacking heterozygotes altogether are removed from the analysis as uninformative about the magnitude of departure from Hardy-Weinberg proportions. This class includes loci that are monomorphic (comprising a single allele) and also loci that are polymorphic (comprising more than one allele). In addition to reducing sample size, the discarding of such highly informative loci may contribute to the loss of accuracy of RMES (David et al., 2007) for high rates of selfing (Figure 2).

In contrast, our method derives information from all loci. Like most coalescence-based models, ours accounts for the level of variation as well as the way in which it is partitioned within the sample. Even a monomorphic within a sample provides information about the age of the most recent common ancestor of the observed sequences relative to the rate of mutation, a property that was not widely appreciated until analyses of variation on human Y chromosomes (Dorit et al., 1995; Fu and Li, 1996). Further, observation of only homozygotes at a polymorphic locus provides strong support for high rates of inbreeding.

By determining likelihoods through the Ewens Sampling Formula (ESF), our method preserves information about the number of allelic classes and the multiplicity of each genotype in the sample. We connect the sample of genotypes, in which up to 2 alleles per locus may be observed in each individual, to the ESF by integrating over genealogical histories back to the point at which all lineages occur in distinct individuals. At this point, the ESF provides the exact likelihood, obviating the need for further genealogical reconstruction. This approach permits computationally efficient analysis of large samples of individuals with large numbers of observed loci across the genome.

Our method provides a posterior distribution of the number of consecutive generations since the most recent outcrossing event in the ancestry of each individual ( $T_k$  for individual  $k$ ). This event, shared by all gene genealogies across the genome, gives rise to identity disequilibrium (Cockerham and Weir, 1968). Conditional on the time since the most recent outcrossing event, genealogical histories across loci are independent. David et al. (2007) seek to approximate the likelihood by summing over the time since the most recent outcross event, but for practical reasons truncate the sum at 20 generations. Our method explicitly estimates the latent variable of time since the most recent outcross for each individual. For any individual, this quantity may range over the non-negative integers, but values are explored by the MCMC according to their effects on the likelihood.

## 5.2 Frequentist coverage properties

Bayesian approaches afford a direct means of assessing confidence in parameter estimates. Our simulation studies suggest that our method obtains Bayesian credible intervals with relatively good frequentist coverage properties.

However, the confidence intervals reported by the **RMES** software package for the maximum-likelihood method of David et al. (2007) appear to perform less well (Fig. 5). David et al. (2007) determine confidence intervals via the profile likelihood method, which should perform well for models with likelihoods that are functions of single parameters and with parabolic likelihood surfaces. In contrast, the likelihood function used by **RMES** depends on multiple parameters. To determine the likelihood profile of the rate of selfing ( $s$ ), David et al. (2007) recommend holding the other parameters constant. However, the **RMES** package holds constant not the apparent heterozygosity ( $d_l$ ) but

$$\frac{d_l}{1-f} = \frac{d_l(1-s/2)}{1-s},$$

for  $f$  the coefficient of identity, a quantity thought to be less correlated with  $s$ .

## 5.3 Model fit

Bayesian approaches also permit insight into the suitability of the underlying model. Our method provides estimates of the number of generations since the most recent outcross event in the immediate ancestry of each individual ( $T$ ). We can pool such estimates of selfing times to obtain an empirical distribution of the number of selfing generations, a procedure particularly useful for samples containing observation of the genotype of many individuals. Under the assumption of a single population-wide rate of self-fertilization, we expect selfing time to have a geometric distribution with parameter corresponding to the estimated selfing rate (Fig. 7). Empirical distributions of the estimated number of generations since the last outcross appear consistent with this expectation for the PG *K. marmoratus* population (Fig. 15) and for Schiedea (Fig. 19). In contrast, the empirical distribution for the highly-inbred BP *K. marmoratus* population (Fig. 11) shows an absence of individuals formed by random outcrossing ( $T = 0$ ). This discrepancy may indicate a departure from the underlying model, which assumes reproduction either through self-fertilization or through random outcrossing. In particular, high rates of biparental inbreeding as well as selfing may reduce the fraction

of individuals formed by random outcrossing. Mis-scoring of heterozygotes as homozygotes due to null alleles or other factors can also in principle contribute to the paucity of outbred individuals.

## 5.4 Comprehensive characterization of mating systems

Our analysis of pure hermaphroditism, androdioecy, and gynodioecy indicates that the probability of an observed genotypic spectrum depends on just two composite parameters: the probability that a random individual is uniparental ( $s^*$ ) and the scaled rate of mutation  $\theta^*$  (9), which reflects the rate of parent-sharing ( $1/N^*$ ). Depending on the mating system, several basic parameters may influence these composite parameters: for example, the gynodioecy model includes the viability of inbred offspring relative to outbred offspring, the proportion of hermaphrodites among reproductives, and the rate of seed set by male-steriles relative to hermaphrodites. Such parameters are nonidentifiable in that any set that determine the same values of  $s^*$  and  $\theta^*$  have the same likelihood.

Our implementation of our inference method explicitly incorporates the full set of parameters for each mating system. By allowing inference on possibly nonidentifiable parameters, this feature introduces the possibility of using information of various kinds in addition to the genotype data. In particular, incorporation of observations on the proportions of males and hermaphrodites into our analysis of the *K. marmoratus* data permitted the joint estimation of the uniparental fraction  $s^*$  and the proportion of males. Empirical data on the intensity of inbreeding depression would permit inference of the proportion of self-fertilization events. Our analysis of gynodioecious *Schiedea* introduced previous experimental results on inbreeding depression through the prior distribution for the relative viability of inbred offspring ( $\tau$ ), permitting inference about the fraction of seeds of hermaphrodites that are set by self-pollen (Table 1). A comprehensive analysis, incorporating a joint likelihood across multiple kinds of observations, would allow characterization of various aspects of the mating system in addition to the rate of self-fertilization.

## 6 Acknowledgments

### References

- Ayres KL, Balding DJ. 1998. Measuring departures from Hardy-Weinberg: a Markov chain Monte Carlo method for estimating the inbreeding coefficient. *Heredity*. 80:769–777.
- Clegg MT. 1980. Measuring plant mating systems. *Bioscience*. 30:814–818.
- Cockerham CC, Weir BS. 1968. Sib mating with two linked loci. *Genetics*. 60:629–640.
- David P, Pujol B, Viard F, Castella V, Goudet J. 2007. Reliable selfing rate estimates from imperfect population genetic data. *Mol Ecol*. 16:2474–2487.
- Dorit RL, Akashi H, Gilbert W. 1995. Absence of polymorphism at the ZFY locus on the human Y chromosome. *Science*. 286:1183–1185.

- Enjalbert J, David JL. 2000. Inferring recent outcrossing rates using multilocus individual heterozygosity: application to evolving wheat populations. *Genetics*. 156:1973–1982.
- Ewens WJ. 1972. The sampling theory of selectively neutral alleles. *Theoretical population biology*. 3:87–112.
- Fu YX. 1997. Coalescent theory for a partially selfing population. *Genetics*. 146:1489–1499.
- Fu YX, Li WH. 1996. Absence of polymorphism at the ZFY locus on the human Y chromosome. *Science*. 272:1356–1357.
- Gao H, Williamson S, Bustamante CD. 2007. A markov chain monte carlo approach for joint inference of population structure and inbreeding rates from multilocus genotype data. *Genetics*. 176:1635–1651.
- Haldane J. 1924. A mathematical theory of natural and artificial selection. part ii the influence of partial self-fertilisation, inbreeding, assortative mating, and selective fertilisation on the composition of mendelian populations, and on natural selection. *Biological Reviews*. 1:158–163.
- Hill WG, Babiker HA, Ranford-Cartwright LC, Walliker D. 1995. Estimation of inbreeding coefficients from genotypic data on multiple alleles, and application to estimation of clonality in malaria parasites. *Genet. Res.* 65:53–61.
- Karlin S, McGregor J. 1972. Addendum to a paper of w. ewens. *Theoretical Population Biology*. 3:113–116.
- Nordborg M, Donnelly P. 1997. The coalescent process with selfing. *Genetics*. 146:1185–1195.
- Pritchard JK, Stephens M, Donnelly P. 2000. Inference of population structure using multilocus genotype data. *Genetics*. 155:945–959.
- Ritland K. 2002. Extensions of models for the estimation of mating systems using n independent loci. *Heredity*. 88:221–228.
- Sakai AK, Karoly K, Weller SG. 1989. Inbreeding depression in *Schiedea globosa* and *S. salicaria* (Caryophyllaceae), subdioecious and gynodioecious Hawaiian species. *American Journal of Botany*. pp. 437–444.
- Wang J, EL-KASSABY YA, Ritland K. 2012. Estimating selfing rates from reconstructed pedigrees using multilocus genotype data. *Molecular ecology*. 21:100–116.
- Wright S. 1921. Systems of mating. i, ii, iii, iv, v. *Genetics*. 6:111–178.
- Wright S. 1969. *Evolution and the Genetics of Populations, Vol. 2, The Theory of Gene Frequencies*. Chicago: Univ. Chicago Press.

## A Uniparental proportion and rate of parent-sharing

For the mating systems of pure hermaphroditism, androdioecy, and gynodioecy, we provide expressions for the probability that a random individual is uniparental ( $s^*$ ) and the probability that a pair of genes sampled from distinct individuals derive from the same individual in the immediately preceding generation ( $1/N^*$ ).

### A.1 Pure hermaphroditism

Each generation,  $N_h$  reproductives generate offspring, of which a proportion  $\tilde{s}$  at conception are uniparental.

**Uniparental proportion:** We assume that the magnitude of inbreeding or outbreeding depression depends only on the reproductive mode through which offspring are derived. The probability that a random individual is uniparental ( $s^*$ ) corresponds to the fraction of uniparentals among surviving offspring:

$$s_H = \frac{\tilde{s}\tau}{\tilde{s}\tau + 1 - \tilde{s}}$$

(see (1a)), for  $\tau$  the rate of survival of a uniparental zygote relative to a biparental zygote.

**Parent-sharing:** We address  $1/N^*$ , the probability that two genes, each sampled from a random individual, derive from the same individual in the immediately preceding generation. In the case in which the individuals bearing the sampled genes are both uniparental (probability  $s_H^2$ ), they share their parent with probability  $1/N_h$  and the pair of genes are derived from that parent with probability 1. For genes sampled from two biparental individuals (probability  $(1 - s_H)^2$ ), the individuals share exactly 1 parent with probability

$$\frac{\binom{2}{1} \binom{N_h-2}{1}}{\binom{N_h}{2}} = \frac{4}{N_h} + o\left(\frac{1}{N_h}\right),$$

and 2 parents with a probability of smaller order. Both genes derive from the common parent with probability  $1/4$ . In the remaining case (genes from a uniparental and a biparental individual), the individuals share a parent with probability

$$\frac{\binom{1}{1} \binom{N_h-1}{1}}{\binom{N_h}{2}} = \frac{2}{N_h},$$

and both genes derive from that parent with probability  $1/2$ .

We address the probability that two genes, each sampled from a random individual, derive from the same individual in the immediately preceding generation. In the case in which the individuals bearing the sampled genes are both uniparental (probability  $s_H^2$ ), they share their parent with probability  $1/N_h$  and the pair of genes are derived from that parent with probability 1. For a pair of genes pair both sampled from biparental individuals (probability

$(1 - s_H)^2$ ), they share their parent with probability  $1/N_h$  and the pair of genes are derived from that parent with probability 1.

To order  $1/N_h$ , the total probability that a pair of genes sampled from distinct individuals derive from the same parent ( $1/N^*$ ) is given by (1b):

$$1/N_H = [s_H^2 + 4s_H(1 - s_H)(1/2) + 4(1 - s_H)^2(1/4)] / N_h = 1/N_h.$$

For this model, we assign the arbitrary constant  $N$  in (7) as  $N_h$ , implying  $c = 1$ .

## A.2 Androdioecy

The reproductive population comprises  $N_h$  hermaphrodites and  $N_m$  males. A proportion  $\tilde{s}$  of broods derive from self-fertilization and the complement from fertilization by males.

**Uniparental proportion:** The proportion ( $s^*$ ) of individuals that are uniparental (2a) is identical to the case of pure hermaphroditism (1a).

**Parent-sharing:** Under androdioecy, all maternal parents are hermaphroditic. A pair of uniparental individuals share their parent with probability

$$\frac{1}{N_h}. \quad (\text{A.1a})$$

A uniparental individual and a biparental individual share a parent with this probability as well. A pair of biparental individuals share their maternal parent but not their paternal parent with probability

$$\frac{N_m - 1}{N_h N_m}, \quad (\text{A.1b})$$

and only their paternal parent with probability

$$\frac{N_h - 1}{N_h N_m}. \quad (\text{A.1c})$$

Assuming negligible probabilities of sharing of more than one parent by two offspring or sharing of a parent by more than two offspring, we obtain the probability (2b) that a pair of genes sampled from distinct individuals derive from the same parent ( $1/N^*$ ):

$$\begin{aligned} \frac{1}{N_A} &= s_A^2 \frac{1}{N_h} + 2s_A(1 - s_A) \frac{1}{2N_h} + (1 - s_A)^2 \left( \frac{1}{4N_h} + \frac{1}{4N_m} \right) \\ &= \frac{(1 + s_A)^2}{4N_h} + \frac{(1 - s_A)^2}{4N_m}. \end{aligned}$$

Unlike the case of pure hermaphroditism (1a), the rate of parent-sharing under androdioecy depends upon the uniparental proportion  $s_A$ .

We assign the arbitrary constant  $N$  in (7) as  $(N_h + N_m)$ , implying a scaled rate of coalescence of

$$c = \frac{(1 + s_A)^2}{4(1 - \rho_m)} + \frac{(1 - s_A)^2}{4\rho_m},$$

for

$$\rho_m = \frac{N_m}{N_h + N_m} \quad (\text{A.2})$$

the proportion of males among reproductive individuals.

### A.3 Gynodioecy

Seed parents comprise  $N_f$  females and  $N_h$  hermaphrodites, with each female generating seeds at rate  $\sigma$  relative to each hermaphrodite. Females set all seeds from the population pollen cloud, which derives entirely from hermaphrodites. Hermaphrodites set a proportion  $a$  of their seeds by self-pollen and the remaining proportion from the population pollen cloud. Of biparental offspring (those derived from the pollen cloud), a proportion  $H$  (4) have a hermaphroditic seed parent and the complement a female seed parent.

**Uniparental proportion:** Ignoring terms of order  $1/N_f$  or  $1/N_h$ , the uniparental proportion  $s^*$  corresponds to (3a):

$$s_G = \frac{\tau N_h a}{\tau N_h a + N_h(1 - a) + N_f \sigma},$$

for  $\tau$  the rate of survival of uniparental offspring relative to biparental offspring.

**Parent-sharing:** A pair of uniparental individuals share their parent with probability  $1/N_h$ . A uniparental individual and a biparental individual share a parent with probability

$$H \frac{2}{N_h} + (1 - H) \frac{1}{N_h},$$

and two biparental individuals share exactly one parent with probability

$$H^2 \frac{4}{N_h} + 2H(1 - H) \frac{2}{N_h} + (1 - H)^2 \left[ \frac{1}{N_f} + \frac{1}{N_h} \right], \quad (\text{A.3})$$

for  $H$  given by (4). In total, the probability that a pair of genes sampled from distinct individuals derive from the same parent ( $1/N^*$ ) corresponds to (3b):

$$\begin{aligned} \frac{1}{N_G} &= s_G^2 \frac{1}{N_h} + s_G(1 - s_G)(1 + H) \frac{1}{N_h} + (1 - s_G)^2 \left[ \frac{(1 + H)^2}{4N_h} + \frac{(1 - H)^2}{4N_f} \right] \\ &= \frac{[2 - (1 - s_G)(1 + H)]^2}{4N_h} + \frac{[(1 - s_G)(1 - H)]^2}{4N_f}. \end{aligned}$$

This expression depends on both the fraction of uniparental offspring ( $s_G$ ) and the proportion of biparental offspring with a hermaphroditic seed parent ( $H$ ).

We assign the arbitrary constant  $N$  in (7) as  $(N_h + N_f)$ , implying a scaled rate of coalescence of

$$c = \frac{[2 - (1 - s_G)(1 + H)]^2}{4(1 - \rho_f)} + \frac{[(1 - s_G)(1 - H)]^2}{4\rho_f},$$

for

$$\rho_f = \frac{N_f}{N_h + N_f} \quad (\text{A.4})$$

the proportion of females (male-steriles) among reproductive individuals.

## B Implementation of the MCMC

### B.1 Efficient inference on selfing times through dynamic programming proposals

Simple Metropolis-Hastings (MH) proposals for  $T_k$  lead to extremely poor mixing efficiency. This is because the selfing time  $T_k$  and the coalescence indicators  $I_k$  are strongly correlated, so that changes to  $T_k$  will be rejected unless  $I_k$  is updated as well. For example, consider proposing a change of  $T_k$  from 1 to 0. When  $T_k = 1$ , on average half the  $I_{lk}$  will be 1 and half will be 0.  $T_k = 0$  will always be rejected if any of the  $I_{lk} = 1$ , since the probability of a coalescence during selfing is 0 when there is no selfing. We therefore introduce a proposal for  $T_k$  that also changes  $I_k$  so that changes to  $T_k$  may be accepted.

The proposal starts from the value  $T_k = t_k$  and proposes a new value  $t'_k$ . In standard MH within Gibbs, we would compute the probability of  $T_k = t_k$  and of  $T_k = t'_k$  given that all other parameters are unchanged. We modify this MH scheme to compute probabilities without conditioning on the coalescence indicators for individual  $k$ . However, the coalescence indicators for other individuals are still held constant. To compute this probability, let  $\mathbf{J}$  indicate all the coalescence indicators  $I_{.y}$  where  $y \neq k$ . Then

$$\Pr(\mathbf{X}, \mathbf{T}, \mathbf{J}, s, \theta) = \Pr(\mathbf{X}, \mathbf{J} | \mathbf{T}, s, \theta) \Pr(\mathbf{T} | s) \Pr(s) \Pr(\theta).$$

We introduce  $\mathbf{I}_k$  by summing over all possible values  $\mathbf{i}_k$ .

$$\Pr(\mathbf{X}, \mathbf{J} | \mathbf{T}, s, \theta) = \sum_{\mathbf{i}_k} \Pr(\mathbf{X}, \mathbf{I}_k = \mathbf{i}_k, \mathbf{J} | \mathbf{T}, s, \theta).$$

Since the  $i_{lk}$  for different loci are independent given  $T_k$ , we have

$$\begin{aligned} \Pr(\mathbf{X}, \mathbf{J} | \mathbf{T}, s, \theta) &= \sum_{\mathbf{i}_k} \prod_{l=1}^L \Pr(\mathbf{X}_l, I_{lk} = i_{lk}, \mathbf{J}_l | \mathbf{T}, s, \theta) \\ &= \prod_{l=1}^L \sum_{i_{lk}} \Pr(\mathbf{X}_l, \mathbf{I}_{lk} = i_{lk}, \mathbf{J}_l | \mathbf{T}, s, \theta). \end{aligned}$$

Therefore, for specific values of  $\mathbf{T}$  and  $\mathbf{J}$ , we can compute the sum over all possible values of  $\mathbf{I}_k$  for  $l = 1 \dots L$  in computation time proportional to  $L$  instead of  $2^L$ . This is possible because the  $L$  coalescence indicators for individual  $k$  each affect different loci, and are conditionally independent given  $T_k$  and  $\mathbf{J}$ .

After accepting or rejecting the new value of  $T_k$  with  $I_k$  integrated out, we must choose new values for  $\mathbf{I}_k$  given the chosen value of  $T_k$ . Because of their conditional independence, we may separately sample each coalescence indicator  $I_{lk}$  for  $l = 1 \dots L$  from its full conditional given the chosen value of  $T_k$ . This completes the collapsed MH proposal.



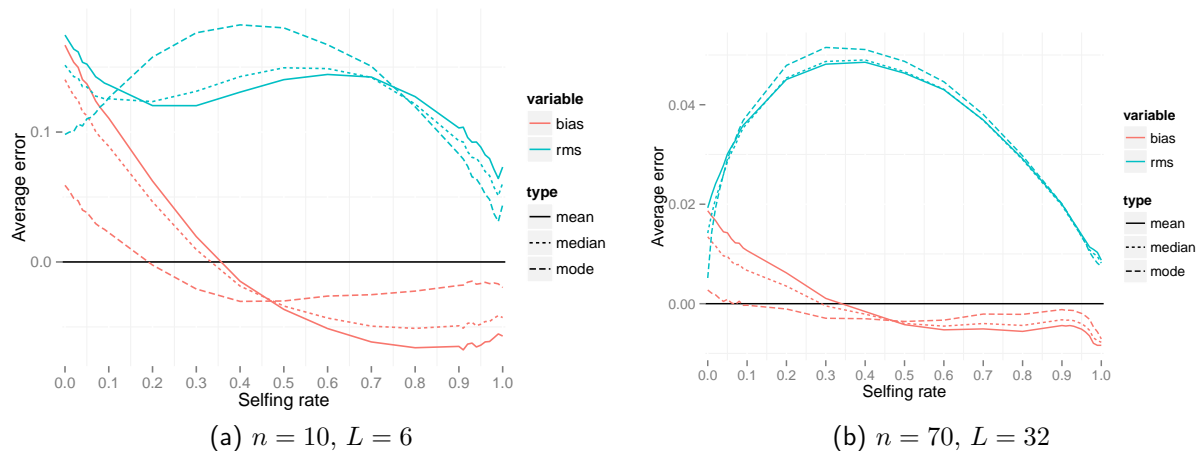


Fig. 20: Errors for the posterior mean, posterior median, and posterior mode. RMES indicates the root-mean-squared error, while bias indicates the average deviation. Averages are taken across simulated data sets at each true value of the selfing rate  $s^*$ .

## C Results

### C.1 Errors

#### C.1.1 Different ways of reporting error in the posterior distribution

When we seek to characterize the accuracy of the posterior distribution, we previously reported the accuracy of the posterior median. Collapsing the posterior distribution to a point estimate allows for comparison with ML methods that report only a point estimate. However, there is more than one way to obtain a point estimate from the posterior distribution. Figure 20 illustrates the root-mean-squared error of the posterior mean, posterior median, and posterior mode. These different measures have substantially different properties. Specifically, the posterior mode shows a much smaller bias than the other point estimates, but shows a high degree of error when  $s^*$  is not near the boundaries of 0 or 1. The differences between these point estimates shows that, while each point estimate is informative, none of them fully characterizes the posterior distribution. Therefore the results should be taken with caution.